Proc. of SPIE Vol. 2264, Vibration Monitoring and Control, ed. C G Gordon (Oct 1994) Copyright SPIE

A PRACTICAL PRODUCT IMPLEMENTATION OF AN ACTIVE/PASSIVE VIBRATION ISOLATION SYSTEM

A.M BEARD, Ph. D., M.E.
D.W. SCHUBERT, M.S., M.E.
Barry Controls, Brighton, MA

A. H. von Flotow Ph D. M.E
Hood Technology Corporation, Hood River, OR

ABSTRACT

A hybrid active-passive vibration isolation system is considered for isolating sensitive payloads from seismic level base disturbances and payload induced force disturbances. Stability robustness requirements justify a detailed investigation of system dynamics, highlighting physical consequences of conventional actively enhanced soft mounting. The proposed "hard-mount" strategy provides desired performance and stability robustness, confirmed by theoretical and experimental results.[1]

NOTATION

F_d, V_{in}	payload and base disturbances respectively
V_p, V_1, V_2, V_r	inertial velocities
k, k_a, k_1, k_2, k_r	system stiffnesses
R, ζ	damping coefficient and ratio respectively
F_c, δ_c	controlled force and displacement respectively
S_p, S_v	payload and disturbance spectral densities
m, m_1, m_2, m_p, m_r	system masses
ω_p, ω_o	parasitic resonance and notch frequencies respectively.

INTRODUCTION

Seismic floor inputs produce unacceptably high vibration levels for sensitive manufacturing and measuring operations. Typically little can be done to reduce support motions short of costly and inflexible approaches such as pouring oversized foundations. The presence of vehicle and foot traffic, as well as manufacturing operations, necessitate reducing transmitted, rather than source, vibration. Although the user may have control of payload force disturbances and mount flanking paths, both payload and base disturbances are usually significant. For some applications the disturbance might be as small as the forces developed by payload interaction with ambient air motion.

Traditionally, attenuation of transmitted support motion is achieved using mounts with natural frequencies well below the lowest disturbance frequency of interest. In the case of seismic floor vibration, it is desirable to provide isolation beginning at 1 Hz. Typically desired seismic isolation cannot be achieved with passive technology, due to low frequency disturbance content, mount amplification, and the negative impact of relative velocity damping on high frequency transmissibility. Active enhancement of traditional low frequency mount dynamics is one approach to achieve desired isolation. Similar to purely passive approaches this method is not very well suited to rejecting payload disturbances, due to soft mounting. Perhaps more importantly, tuning of the active feedback-enhanced soft mount is payload dependent. The coupling of payload modes with sensors adversely affects stability robustness requiring compensator tuning specific to payload dynamics.

[1] Similar paper presented to the IUTAM Symposium on the Active Control and Vibration, University of Bath, UK, September 5 - 8, 1994.

With appropriate actuator/sensor pairing, base disturbance rejection can be achieved actively, enabling the use of hard passive mounting to improve payload disturbance rejection while providing decoupling from uncertain payload dynamics, needed for stability robustness. Such an isolation system enhances the rejection of base and payload disturbances, with minimal sensitivity to payload and support structure dynamics. This paper examines the physical consequences of traditional passive and actively enhanced "soft mounts" providing justification for the development of a hard mount concept. Documenting the development of a hard mount isolation system, this paper covers theoretical and laboratory developments.

PASSIVE SOFT MOUNT

Simplistically considered as a rigid body, an isolated payload has six degrees-of -freedom (dof) and a complete description of payload motion requires modeling as such. For purposes of illustration however, single dof modeling is sufficient. Figure 1 schematically represents a passively mounted payload subjected to a base velocity disturbance, Vin, and a payload force disturbance, Fd. The system responses to these disturbances, assuming the system to be linear, are given by transfer functions, rational functions of the Laplace variable s. For the stable platform application considered, absolute payload velocity, Vp, is the output to be minimized. Equation (1) and eqn. (2) depict these responses respectively, where ω_n is the mount natural frequency and ζ the fraction of critical damping ($k/m = \omega_n^2$, $R/m = 2\zeta\omega_n$).

$$\frac{V_p}{V_{in}} = \frac{2\zeta\omega_n s + \omega_n^2}{s^2 + 2\zeta\omega_n s + \omega_n^2} \tag{1}$$

$$\frac{V_p}{F_d} = \frac{s/m}{s^2 + 2\zeta\omega_n s + \omega_n^2} \tag{2}$$

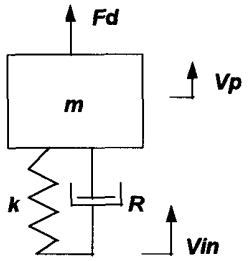

Figure 1 Single dof model of passive isolator indicating base velocity and payload force disturbances

Overall mount effectiveness depends on the isolator transfer functions and a spectral description of the disturbances. The contribution of base motion to payload velocity power spectral density is illustrated by eqn. (3), where S_v is the base disturbance PSD and S_p is the payload motion PSD. An analogous equation exists for payload disturbances.

$$S_p = S_v \left| \frac{V_p}{V_{in}}(s) \right|^2 \tag{3}$$

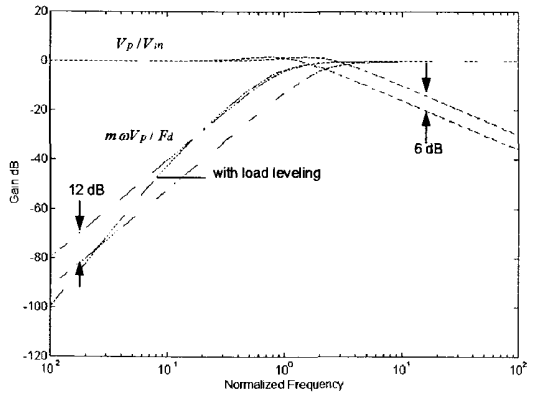

a)

Figure 2 a) Trade-off between base and payload disturbance rejection as ω_n is changed from one to two.

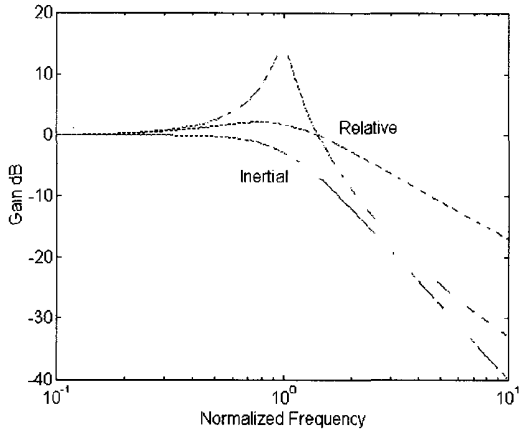

b)

Figure 2 b) Impact of "high" and "low" relative velocity damping on asymptotic isolation compared to equal "high" inertial damping.

As a dimensionless plot of eqn. (1) and eqn. (2), Fig. 2a serves to illustrate a fundamental limitation of passive isolation methods. Improved rejection of base disturbances comes at the expense of payload disturbance rejection and vice-versa. Figure 2a illustrates that a factor of two reduction in mount natural frequency provides 6 dB more base disturbance isolation above resonance This improved isolation comes at the expense of 12 dB reduced force disturbance isolation below mount resonance. Furthermore, increased base disturbance rejection around mount resonance using relative velocity damping compromises isolation above resonance, Fig. 2b. Due to practical isolator size constraints and the trade-offs made between rejecting payload and base disturbances, passive stable platform resonance is typically above 1 Hz. The desire for isolation at this frequency motivates high damping, but as eqn. (1) suggests the transmissibility function is greater than one for $\omega < 1.4\omega_n$, in addition to the higher frequency penalty paid for relative velocity damping. The physical and practical limitations of passive isolators motivate active damping.

ACTIVELY ENHANCED SOFT MOUNT

The damper depicted in Fig. 1 generates forces proportional to the relative velocity across it, producing a zero in eqn. (1) that is damping dependent. Where damping forces are proportional to absolute payload motion, always opposing payload motion, there is no high frequency penalty paid for increased damping. Depicted passively in Fig. 3a and suggested as an active realization in Fig 3b, inertial or "skyhook" (1) damping results in the transmissibility function of eqn. (4) Given the constraints on system performance using relative velocity damping, an actively damped soft mount is a natural extension of passive technology.

$$\frac{V_p}{V_{in}} = \frac{\omega_n^2}{s^2 + 2\zeta\omega_n s + \omega_n^2} \tag{4}$$

Inertial damping enables transmissibilities less than unity at, and below, the mount natural frequency, without any degradation of high frequency asymptotic behavior. Figure 2b illustrates the advantage of inertial damping compared to equal relative velocity damping, for rejecting base disturbances. Force actuation depicted in Fig. 3b may be achieved directly, such as with a voice-coil actuator, or with a displacement actuator in series with a compliant element, such as a piezo-ceramic stack and elastomer bushing. Inertial damping, in conjunction with load leveling control, typical even on passive pneumatic isolators, overcomes some of the shortcomings of soft passive mountings.

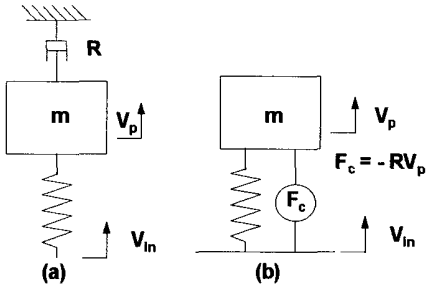

Figure 3 a) Passive and active, b), implementations of inertial damping. Active realization requires sensing V_p.

Sensitivity to payload disturbances can be suppressed at low frequencies with the addition of a low bandwidth load leveling loop, Fig. 2a.. Commonly, mechanical sensing of sway space is used to limit static deflection independent of payload weight **(2).** Issues such as sensitivity to sensor noise, actuation power requirements, and saturation levels prevent the leveling loop bandwidth from approaching the mount frequency ($\omega_b \approx \omega_n / 10$). Consequently soft mount stable platforms suffer from the physical limitations illustrated by Fig. 2., a trade-off between payload and base disturbance rejection.

PRACTICAL DESIGN ISSUES

The physical consequences of active soft mounting extend beyond compromised payload disturbance rejection. Although conveniently modeled as a single rigid body, payload dynamics become relevant within the active damping bandwidth for most realistic payloads. Stability concerns associated with feedback control require that the active bandwidth must not exceed that for which the system dynamics are understood. Figure 4a suggests the most simple representation of flexible payload dynamics.

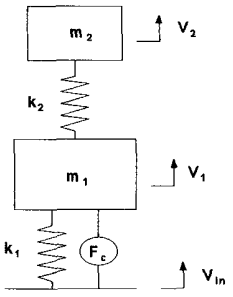

Figure 4a) Simple model used to investigate effect of payload dynamics on loop transfer functions.

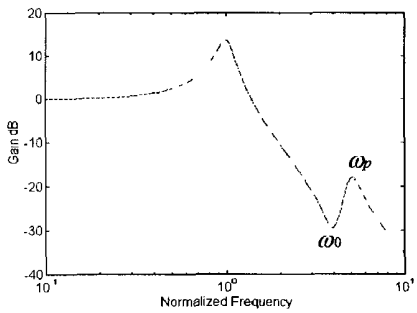

Figure 4b) Illustration of coupling of payload mode to sensed output.

For the case of force actuated inertial damping the plant transfer function relates payload velocity, V_1, to control force, F_c, as shown in eqn. (5). Figure 4b illustrates that the added degree of freedom introduces pole-zero pairs into the plant, and therefore the loop transfer function. For soft mounting, where the "parasitic" eigenfrequency is greater than the mount frequency, the zeros come before the poles, as shown in Fig. 4b. Although the resulting phase lead does not compromise stability, the associated gain increase does Gain margin is compromised by resonance and the step increase in gain due to this "lead" network. Resonance magnitude is determined by modal damping, and the increase in asymptote gain is dependent on the frequency separation between zeros and poles. **(3)** Pole-zero separation is proportional to mode coupling strength and should be minimal for stability robustness. Equation (5) clearly indicates zero locations, ω_b. Assuming the mount (k_1, m_1) is mass controlled, pole locations are well approximated by eqn (6).

$$\frac{V_1}{F_c} = \frac{\frac{s}{m_1}(s^2 + \frac{k_2}{m_2})}{s^4 + (\frac{k_2}{m_2} + \frac{(k_1+k_2)}{m_1})s^2 + \frac{k_1 k_2}{m_1 m_2}} \tag{5}$$

$$\omega_p{}^2 \approx \frac{k_2(m_2+m_1)}{m_1 m_2} = \omega_0{}^2(1+\frac{m_2}{m_1}) \tag{6}$$

Coupling strength of payload modes with a chosen sensor is determined by plant pole-zero separation. Equivalently, the asymptote gain change, GC_s ,due to the payload mode is given by eqn. (7). This relationship indicates a strong dependence of stability robustness on payload dynamics for soft mounting, given that both payload mass, m_1, and payload modal mass, m_2, are characteristics of the payload, not the mounting.

$$GC_s = 20\log(1+\frac{m_2}{m_1}) \tag{7}$$

Strong coupling within the open loop bandwidth requires application specific compensator tuning to achieve desired performance and stability. To minimize compensator complexity, and sensitivity to payload dynamics, actuator-sensor pairing should address the coupling strength of payload dynamics with sensed outputs.

ACTIVE HARD MOUNT

Figure 5 illustrates an active-passive alternative to inertially damped soft mounting. Payload mass, m_p, is supported on a passive mount of stiffness k_p, chosen to realize a resonant frequency an order of magnitude greater than typical soft mounting, about 20 Hz. Base disturbance, V_{in}, rejection is achieved with sensing of the absolute velocity, V_i, of an intermediate mass, m_i, using feedback control As a theoretical ideal, the motion of this mass is controlled by ideal displacement actuation, δ_c, in practice, however, actuator compliance is relevant and accounted for by the stiffness parameter k_a.

Coupling of payload modes with a payload motion sensor is dependent on the mass ratio of eqn. (7) for soft mounting. With the hard mounting scheme worst case coupling is achieved if the payload is considered a rigid body. For this case, coupling strength is estimated by assuming the intermediate mass mode (k_a / m_i) to be stiffness controlled at the passive mount eigenfrequency (k_p / m_p). Consequently the desired pole locations are well approximated by assuming that payload mass resonates on the serial combination of springs.

$$\frac{V_i}{\delta_{in}} = \frac{\frac{k_a}{m_i}(s^2 + \frac{k_p}{m_p})}{s^4 + (\frac{k_p}{m_p} + \frac{(k_a+k_p)}{m_i})s^2 + \frac{k_a k_p}{m_p m_i}} \tag{8}$$

$$GC_h = 20\log(\frac{k_a}{k_a+k_p}) \approx 20\log(1-\frac{k_p}{k_a}) \tag{9}$$

With zero locations apparent from the transfer function of eqn. (8), eqn (9) indicates modal coupling strength. Consequently an important distinction between hard and soft mounting is the ability to predict modal coupling strength in terms of design parameters (k_m,k_a) with hard mounting. Soft mount mode coupling is dependent on uncertain payload dynamics. Using the hard mount configuration, coupling strength is diminished as the payload becomes mass controlled, providing a cleaner plant to control, even with a payload modally dense above the mount frequency.

The single axis hard mount of Fig. 5 offers both performance and stability advantages over a soft mount with inertial feedback. The weak coupling of payload modes to the intermediate mass velocity sensor results in a controller design that does not need to be tuned to specific payloads. In addition to providing stability robustness through mechanical design, the hard mount overcomes another shortcoming of soft mounting. By choosing a passive mount frequency ten times that of a soft mount, payload disturbance rejection is enhanced considerably, eqn. (2).

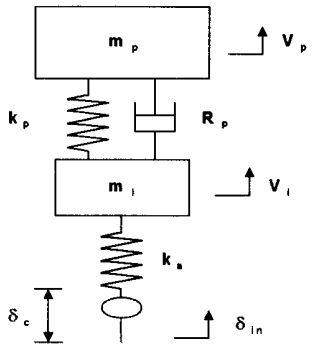

Figure 5 Schematic representation of single axis hard mount.

Numerous factors motivate the use of passive mounting in series with the actively controlled displacement element. Due to the finite stiffness characteristics of actuators, a passive mount, soft compared to the actuator stiffness, is needed to decouple the sensor from the payload, eqn. 9. In addition to providing robustness, a stiff actuator keeps the bounce frequency of the intermediate mass high, preferably outside the desired loop bandwidth. Passive mount compliance provides further stability robustness by enhancing decoupling of the feedback loop from floor compliance. If the intermediate mass is small compared to the effective mass of the floor eigenmode, and the passive mount stiffness is small compared to associated floor stiffness, then the hardmount feedback loop will couple weakly with floor eigenmodes.

Because low order models used to represent system components are only valid for a finite frequency range, and higher order modeling becomes application specific, the hard mount active bandwidth is finite. This provides another motivation for the series passive mount of Fig. 5 Base disturbance isolation continues passively beyond the active bandwidth.

HARD MOUNT DESIGN AND MODELING

Sensitivity to installation specific dynamics, in addition to the need for improved payload disturbance rejection, has motivated development of the hard mount concept of Fig. 5. Unlike soft mounts, which depend on passive element compliance for low frequency base disturbance isolation, the active element of Fig. 5 is primarily responsible for hard mount base disturbance rejection. Utilizing high gain feedback of the intermediate mass motion, the isolation scheme drives this output towards zero, vastly attenuating the input to the passive mount. By nulling the sensed output in the presence of base motions the actuator is accommodating base motions, justifying the designation as a "move-out-of-the-way" isolator.

An ideal displacement actuator is infinitely stiff and capable of controlling displacement independent of load. Although such actuation does not exist, piezo-ceramic actuators behave well enough to be considered for seismic isolation. Capable of .1% actuated strain, these actuators are practically sized to accommodate floor motions up to a milli-inch With nominal vibration magnitudes measured in tens of micro-inches, a one inch long ceramic stack avoids saturation. In addition to providing required displacement, piezo-ceramic stacks meet desired bandwidth specifications, following commanded inputs from DC to beyond one kHz

The intermediate mass of Fig. 5 is required as an actuation interface and sensor housing. To keep the "bounce" frequency of this mass resonating on the actuators that support it outside the loop bandwidth, its mass should be minimized. Housing the sensors that monitor inputs to the passive isolator, block size is influenced by sensor selection. Because piezo actuators control displacement, ideal sensing provides a voltage proportional to absolute block motion. Such an ideal is not practical, but is approximated with a seismometer (4)

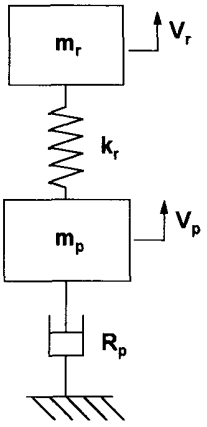

Figure 6 Simple schematic illustration of how mount damping effects payload modes.

The importance of a passive mount in series with the active element has already been introduced. Desired compliance and damping are influenced by the rigid body response of the payload to payload force disturbances, damping of higher order payload modes, decoupling of loop dynamics from the mounting environment, and enhanced base disturbance rejection. As indicated by eqn. (1), high damping is desired for limiting rigid body payload resonance. For payload resonances with eigenfrequencies well above the mount frequency, the characteristic equation of eqn. (11), and Fig. 6 illustrate that mount damping is also desired for attenuating payload modes. Although rigid body payload disturbance rejection motivates stiff passive mounting, eqn. (2), passive enhancement of active base-disturbance isolation, as well as stability concerns are reasons for soft mounting.

$$C.E = s^3 + \frac{R_p}{m_p}s^2 + (\frac{k_r}{m_r} + \frac{k_r}{m_p})s + \frac{k_r R_p}{m_r m_p} \tag{11}$$

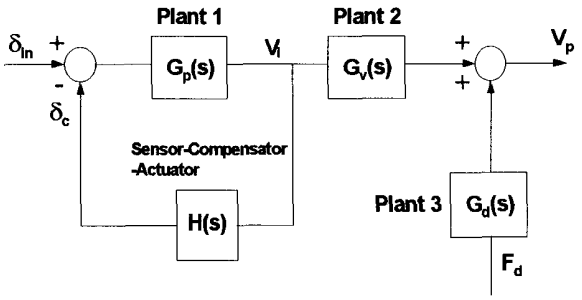

Figure 7 Block diagram representation of active base disturbance rejection control loop.

A nominal mount frequency of 20 Hz. is chosen to meet system stiffness requirements and a damping ratio, ζ, of .2 satisfies damping needs. Elastomeric mounting is chosen as a cost effective way to meet required passive isolation needs.

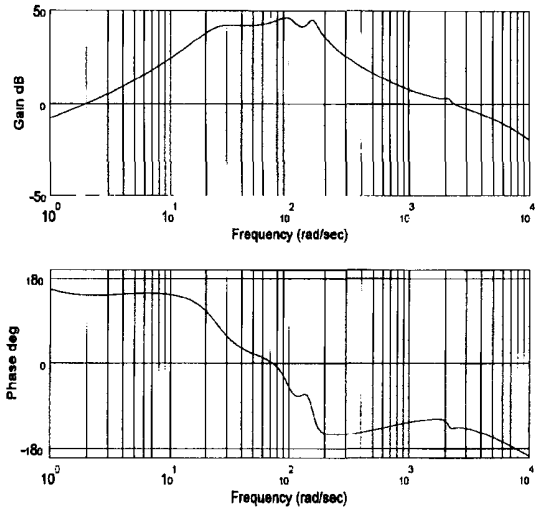

Figure 8 Theoretical open loop transfer function. Relatively stiff passive mounting results in noticeable payload coupling at 150 (rad/sec).

The block diagram of Fig. 7 illustrates the system configuration and control strategy used for single axis isolation, Fig. 5. Characteristic of feedback control, active enhancement of base disturbance rejection requires high loop gain. As indicated by Fig. 8, this loop gain is rolled off such that uncertain system dynamics do not result in instability. Due to sensor dynamics and signal conditioning limitations, the loop has two crossover points and four stability margins. The desire for broadband isolation as well as a high level of isolation motivates a low frequency loop crossover.

An objective of 99 % percent peak active isolation requires that the open loop bandwidth exceed two decades. Depending in part on stability margins, achieving the desired loop gain requires almost three decades of open loop bandwidth A low frequency bound is imposed on the loop crossover frequency by required compensator gain. Given an actuator gain of a micro-inch per Volt, and the low frequency sensor gain characteristics of seismometers, crossover at .3 Hz. requires a maximum compensator gain in the tens of millions. In addition to the voltage and current offset problems imposed by implementing such a high gain with analog circuitry, reduced crossover frequency requires increased filter time constants. Consequently 3 Hz. was chosen as an objective, implying that achieving desired peak loop gain requires a high frequency crossover point around 200 Hz.

To retain stability robustness, the coupling of installation dependent modes must be weak in the loop bandwidth, particularly around crossover. This has been addressed with the passive isolator that decouples the certain dynamics of the isolator from the uncertain dynamics of the payload and floor. Normal modes of the isolator itself also must be addressed to preserve stability. Rigid body motion of the intermediate mass resonating on stack compliance has been mentioned, and includes bounce and rocking modes.

EXPERIMENTAL RESULTS

Loop gain is rolled off before the "rigid" isolator structure breaks up, greatly reducing compensation order and sensitivity to variations in mount dynamics. Because of its proximity to the desired crossover frequency the first isolator mode, bounce of the intermediate mass, is notch compensated. Figure 9 illustrates the experimentally measured loop transfer function Before loop closure the shaped loop of Fig 9 is gain shifted resulting in crossover points at .4 Hz. and 150 Hz.

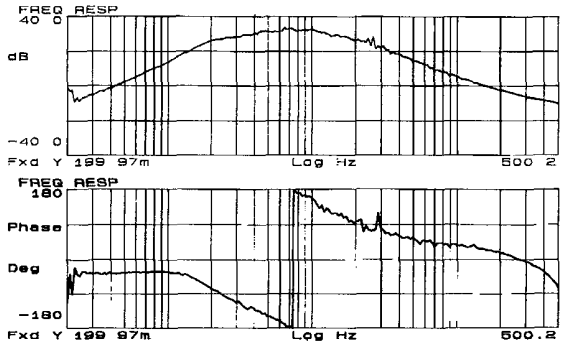

Figure 9 An experimental open loop transfer function. Very weak payload coupling is due to soft (12 Hz.) passive mounting (eqn. 9).

Rapid roll-off of loop gain, resulting in a phase margin of about 40 degrees, is tolerated to improve gain margin, 10 dB. Because the return ratio comes closer to the critical point of minus one on a Nyquist plot at phase (-180 degrees) crossover, rather than gain (0 dB) crossover, gain margin limits overall loop gain. Gain margin is significantly influenced by the higher order isolator modes and phase lag associated with system nonlinearities. Small signal nonlinearities are dominant, particularly drive amplifier crossover distortion.

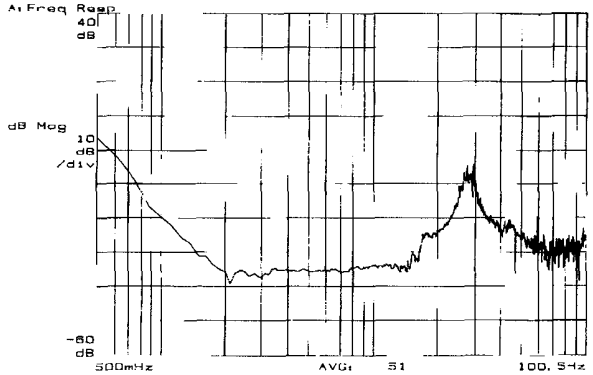

Figure 10 Vertical axis system transmissibility using 27 Hz. passive mounts.

After gain shifting the loop transfer function of Fig. 9, loop closure results in the transfer function of Fig. 10. This transmissibility curve, measured from floor to payload, includes passive mount dynamics. Inherently nonlinear elastomer, mount damping diminishes with attenuated inputs; consequently the passive mount damping ratio is less than 05 with loop closure. It is tempting to use payload inertial velocity feedback to damp the resonance of Fig. 10. As suggested by eqn. 7 and Fig 11, this approach to realizing inertial damping results in strong coupling of payload modes to the sensed output. Because the "lead-lag" networks keep loop gain high, loop closure requires compensation specific to the payload to assure stability.

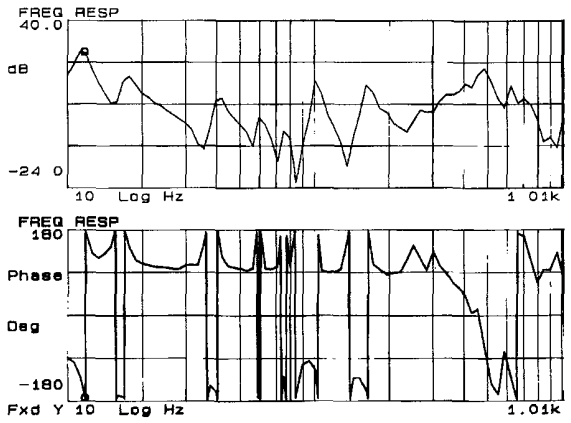

Figure 11 Open loop transfer function sensing payload velocity due to actuator displacement.

Although pole locations are fixed for the dynamic system of interest, zero locations, and therefore coupling strength, depend on the output measured. Choosing an output that results in zeros in close proximity to poles desensitizes the loop to payload dynamics.

Measuring passive mount load or deflection, the inertially damped transmissibility of Fig. 2b is realizable. To investigate mode coupling strength when measuring mount deflection consider the deflection of the spring of stiffness k_1 in Fig 4. For a base input, to be controlled with the piezo actuator, complex zero locations are given by eqn. 12, where passive mount deflection is measured.

$$\omega_0^2 = \frac{k_2(m_2+m_1)}{m_1 m_2} \tag{12}$$

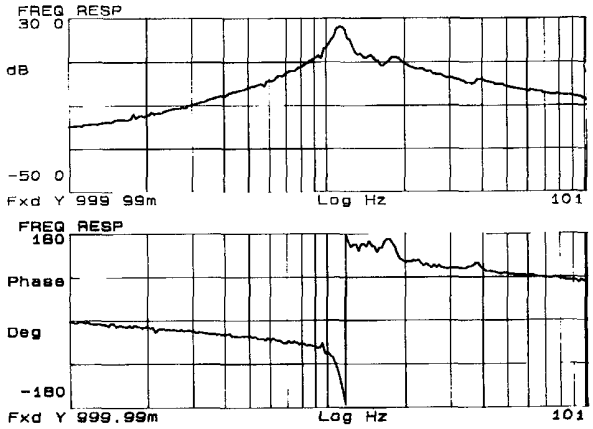

Figure 12 Open loop transfer function sensing relative passive mount deflection due to actuator deflection

Comparison of eqn. 12 with eqn. 6 indicates that poles and zeros are collocated when the passive mount is truly mass controlled. In practice there are payload modes located near the passive mount eigenfrequency and cancellation is not complete, but coupling is weak compared to using payload velocity feedback.

Although only a two dof model was used to illustrate anticipated coupling strength with payload velocity feedback, and weakness with relative displacement feedback, comparison of Fig. 11 and Fig. 12 illustrates the importance of actuator sensor pairing. Figure 12 is the loop transfer function from piezo velocity to measured mount deflection. Without any compensation for payload modes, Fig. 12 can be directly compared to Fig. 11 to illustrate appropriate actuator sensor pairing In particular, notice how weakly payload modes at 17 Hz. and 40 Hz. couple with the displacement sensor compared to the velocity sensor response of Fig. 11. As predicted by the two dof model and eqns 6 and 12, Fig. 12 illustrates that coupling strength diminishes for mode frequencies high compared to the mount frequency. Sensing passive mount deflection, or load, is therefore an appropriate way to incorporate inertial damping into the active mount.

SYSTEM CONFIGURATION

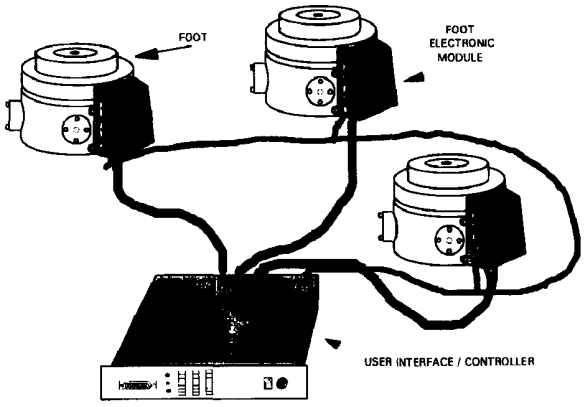

Figure 13 Three foot system configuration.

Figure 5 illustrates the fundamental isolation concept of the single axis hard mount. Six degree-of-freedom payload support is achieved with nine such isolators. As illustrated by Fig. 13, three "feet" are used to support a payload Each "foot" contains the required hardware for three axes of active control. With each axis controlled as a single-input-single-single-output system (SISO), orientation of each foot is not of concern.

Mechanical decoupling of off axis sensors and actuators is mandatory for the SISO control approach taken. Crosstalk between feet is inherently weak due to actuator stiffness, and the relatively soft cup mounts through which "feet" must communicate.

SUMMARY

Improvement upon available seismic isolation systems requires that more attention be paid to system dynamics rather than control theory. Dependence of compensation on uncertain payload dynamics is a fundamental consequence of soft mounting with payload motion feedback.

Attaining good disturbance rejection, from both base motions and payload forces, is attainable with a combination of active and passive isolation techniques. Stability robustness is achieved with simple mechanical components that decouple the modeled isolator dynamics from unmodeled payload dynamics, in the same bandwidth. Further mechanical design efforts enable the use of SISO loops to control the multiple-input-multiple-output system.

Laboratory results indicate that the active hard mount currently provides 75% isolation at 1 Hz and more than 90% isolation by 2 Hz From 5-30 Hz. active isolation is about 98% and passive isolation begins to become effective.

The outer control loop, utilizing mount deflection feedback to achieve inertial damping, improves support motion isolation and transient response to payload disturbances Limited by actuator stroke and high voltage drive, the damping ratio is increased from .05 to about .8. Because this damping is inertial, there is no high frequency penalty paid for attenuating passive mount resonance.

REFERENCES

(1) Karnopp, D C , Crosby, M J , and Harwood, R A "Vibration Control Using Semi-Active Generators," ASME Paper 73-DET-122

(2) Anon Final Engineering Report on Pneumatic Servo-Controlled Vibration Isolation System for ST-90S and ST-125 Stable Platforms Report No 108, (NASA Contract No NAS8-5096), Barry Research and Development Corp , Watertown, Massachusetts, May 1964

(3) Blackwood, Gary H , and von Flotow, Andreas H Active Control for Vibration Isolation Despite Resonant Structural Dynamics A Trade Study of Sensors, Actuators and Configurations Proceedings of the VPI Conference, April 1993

(4) Riedesel, Mark A , Moore, Robert D and Orcutt, John A Limits of Sensitivity of Inertial Seismometers with Velocity Transducers and Electronic Amplifiers Bulletin of the Seismological Society of America, Vol 80, No 6, pp 1725-1752, December 1990